

Viscous Optimization of Interacting Lifting Surfaces

Vincent G. Chapin¹, Yves Caumel²

Institut Supérieur de l'Aéronautique et de l'Espace (ISAE), Toulouse, 31056

Romarc Neyhousser³

Aquitaine Design Team, Arcachon, 33120

In this paper, the optimization of interacting lifting surfaces based on design of experiments (DoE) and response surface technique (RSA) is investigated. Response surfaces of the considered problem are generated through the use of high-fidelity two-dimensional Reynolds Average Navier-Stokes simulations. The large number of simulations necessary to populate response surfaces is obtained by using a newly developed automated simulation platform named *ADONF*[®]. This platform integrate a RANS, URANS flow solver with an automated CAD and mesh generation algorithm and a panel of optimization tools which may be used to generate approximate response surfaces through design of experiments. To gain knowledge about the potential of these tools to resolve non linear fluid flow optimization problems, we have used this simulation environment to study a sailing yacht problem. The aerodynamic performance optimization of complex rigs composed by multiple interacting masts and sails has been investigated. This problem is a well known by sailors because of its crucial importance for high speed sailing yachts and has been a subject of debate and controversy since many years. A new look on this problem is proposed through viscous CFD with parametric and topological optimization. It is a preliminary two-dimensional study with a moderate design space size which will be extended to three dimensional problems and a larger design space size.

I. Introduction

The high applicative value of the optimization techniques to mono and multi-disciplinary design optimization through mono or multi-objectives has not to be demonstrated today (¹Keane, ¹⁴Queipo, ¹⁵Mack, ¹⁷W. Song). A lot of papers are devoted to a small part of this huge research field with many optimization algorithms, DoE techniques and so on but a lot of work is always needed to gain real insight into real complex problems. The application of these techniques to the aerodynamic interaction of lifting surfaces with and without separation regions is always a challenging problem after many years of aeronautical and nautical challenges and innovations. On the aeronautical side, numerous passive solutions have been invented by engineers with multi-elements airfoil systems (slat and flap system, Krueger slat, etc...). On the nautical side, interacting lifting surfaces is an old problem for sailors who try from many years to sail faster by designing interacting sails with a stronger driving interaction. From that point of view, the positive coupling of a mainsail and a jib is a well known subject of controversy (²Marchaj, ^{3,4}Gentry, ⁵Milgram). We should not be surprised when we know that this positive coupling is highly dependent to the presence and extend of separation regions on both sails. Optimization of interacting lifting surfaces can't be definitely resolved without viscous methods and the ability to solve a large number of configurations and designs. These two ingredients are only available since few years (^{6,7}Korpus, ^{11,12}Chapin). It emphasized the interest to reconsider this complex optimization problem in further details. Another motivation is the highly competitive level of multihull ocean racers like the Hydraplaneur of Yves Parlier with which we have worked (⁸Chapin). In 2006, Yves Parlier and the Hydraplaneur have beaten two world sailing speed record ratified by the WSSRC:

- The record of the longest distance run in 24 hours up to 60 foot with 598 nautical miles
- The record of the longest distance run in 24 hours singlehanded with 586 nautical miles

¹Associate Professor, Department of Aerodynamic Energetic and Propulsion, ISAE, vincent.chapin@isae.fr.

²Associate Professor, Department of Mathematics, Informatics and Automatic, ISAE, yves.caumel@isae.fr.

³Chief Designer, Aquitaine Design Team.

One objective of this work was to evaluate the ability of high-fidelity RANS simulations and optimization techniques to search optimal or better designs of interacting lifting surfaces. The second objective was to emphasize physical mechanisms related to the interaction of lifting surfaces in downwind sailing conditions depending to the design space of the problem (sheeting angles, mast angle, sail chord, sails relative position, etc...).

As a first step, optimization will be done for a given single objective with a nonlinear constraint on the heeling moment. During the process described in the following sections, we will illustrate a generic design approach with different phases of increasing complexity toward better designs and also a better understanding of the complex flow field which take place in the studied rig and its evolution through design changes.

II. Test Case Description

In this section, we will give a brief description of the chosen test case which is from the nautical side. It is a modelization of the aerodynamic behaviour of the Hydraplaneur of Yves PARLIER (⁸Chapin & al., 2002). It is an ocean racing multihull yacht which is highly innovative with its twin rig concept. This particular rig is able to generate a highest propulsive force for a given heeling moment than a classical rig. This twin rig is composed by two mainsails and one or two fore sails (figure 1) depending on wind conditions. From the aerodynamic point of view, it is a complex system of two, three or four interacting lifting surfaces. The aerodynamic objective will be to maximize the driving force for a given heeling moment through high lift and low drag of the lifting system. The problem is easy to pose, but the solution is not easy to find. There are a lot of parameters influencing the solution. Design and optimization tools are needed to analyse the large set of solutions and find better ones. One original point of this study is the ability to investigate topological design optimization. Also, the chosen configuration will investigate this interesting capability with a three sails five-variable configuration and a four sails nine-variable configuration. The two mainsails are parameterized by two parameters (sheeting angle and mast angle) and the leeward fore sail by one parameter (sheeting angle). In the second configuration with four sails, the jib1 or windward jib is described by four parameters (chord length, sheeting angle and leading-edge position).

These two configurations have been chosen because of the experience gained in downwind conditions during wind-tunnel tests and true scale tests at sea (⁸Chapin & al., 2002, ^{9,10}Chapin & al., 2005, ¹¹Chapin & al., 2006). These tests have shown advantage of the twin rig concept in upwind conditions and inconvenient in downwind conditions in comparison to classical rigs of ocean racing multihull. The twin rig concept generates flow instabilities when the relative wind angle β is superior to a critical value β_c . This is related to the separated wake interaction of the windward lifting system to the leeward lifting system. This problem has been investigated during sea tests and in windy conditions, the instability of the leeward rig have entrained batten failure in the leeward mainsail.

Two solutions have been investigated and will be presented in this paper. The first one was to optimize the three sails configuration through different approaches. The second one was to replace the three sails configuration by a four sails configuration with an added windward jib to stabilize the flow on the windward rig at high incidence angle (figure 2).



Figure 1: Hydraplaneur twin rig with two mainsails and no jib. (Left) an example of three dimensional mesh for RANS simulations, (center) Hydraplaneur at sea, (right) an example of RANS flow solution

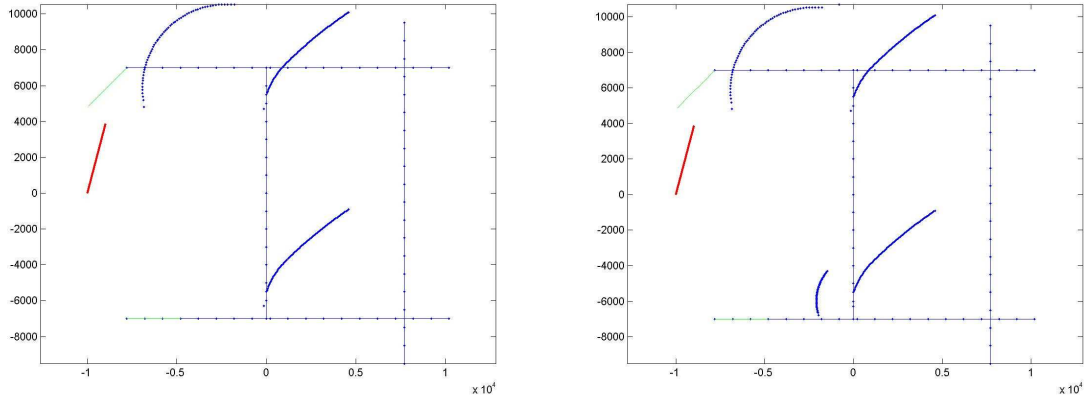


Figure 2: a cut of the three and four sails configurations at the critical apparent wind angle $\beta = 75^\circ$. Red arrow figures apparent wind, blue curves figures the sails and blue lines and points figures the Hydraplaneur platform

III. Parameterization, RANS simulations and validations

A. Parameterization

From the three and four sails configurations of the Hydraplaneur, we may define two parameterizations of the optimization problem. From the sailor point of view they are corresponding to a topological optimization of twin rig concept for downwind conditions. In this paper we have chosen a relative wind angle $\beta=75^\circ$ because it is in the neighbor of the critical angle.

The two chosen parameterizations are the following ones:

- a three sails five-variables (figure 2, 3)
- a four sails nine-variables (figure 2, 3)

The three sails configuration is hence given through the definition of the five parameters in the range of the following table. These parameters are trims angles of the three sails (δ_{GV1} , δ_{GV2} , δ_{P2}) and of the two masts (θ_1 , θ_2). They define the relative position of each components of the rig in the apparent wind.

The four sails configuration is given by the same five parameters of the three sails configurations with a supplement of four parameters to define the position (x_{f1} , y_{f1}) the size (C_{f1}) and the trim angle of the windward jib (δ_{f1}), the fourth sail.

Table 1: three sails five-variable parameterization

	Min	Max	Name, units
δ_{GV1}	40	55	Windward mainsail trim angle, deg
δ_{GV2}	35	50	Leeward mainsail trim angle, deg
δ_{P2}	40	55	Leeward jib trim angle, deg
θ_1	75	95	Windward wing mast trim angle, deg
θ_2	75	95	Leeward wing mast trim angle, deg

Table 2: four sails nine-variable parameterization

	Min	Max	Name, units
δ_{GV1}	40	55	Windward mainsail trim angle, deg

δ_{GV2}	35	50	Leeward mainsail trim angle, deg
δ_{r2}	40	55	Leeward jib trim angle, deg
θ_1	75	95	Windward wing mast trim angle, deg
θ_2	75	95	Leeward wing mast trim angle, deg
x_{f1}	1.5	3.0	Windward jib longitudinal position, m
y_{f1}	4.6	6.6	Windward jib lateral position, m
c_{f1}	2	4	Windward jib chord length, m
δ_{f1}	65	80	Windward jib trim angle, deg

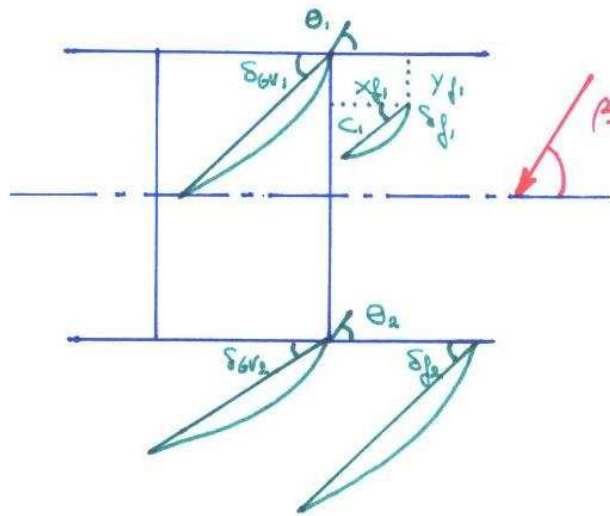


Figure 3: Design space chosen during the optimization process with 5 parameters for three sails configurations and 9 parameters for four sails configurations. Red arrow figures apparent wind, green curves figures the sails and blue lines and points figures the Hydraplaneur platform. Parameters are detailed in Table 1 and 2 for three and four sails configurations.

B. CFD Methodology

All high-fidelity RANS simulations have been done through *ADONF*[®], an automated simulation platform developed at ISAE (¹⁰Chapin 2005, ¹¹Chapin 2006) and based on ¹⁶FLUENT. The principle of *ADONF*[®] is described in figure 4. From an initial design vector, the CAD model construction, mesh generation and solving process are all automated. Based on this core software, a coupling with optimization algorithms is done. With *ADONF*[®] it is then possible to resolve optimization problems through the simulation of the Reynolds Averaged Navier-Stokes equations (RANS). Hybrid meshes are used for flexibility and good quality meshes around bodies for boundary layer prediction. Structured meshes are used around sails and unstructured ones far for sails. Navier-Stokes equations are resolved through second order scheme in space and time. More detailed description and validation of this tool for separated flow around mast and sails, have been presented in ⁹Chapin 2005, ¹⁰Chapin 2005, ¹¹Chapin 2006 for similar geometries.

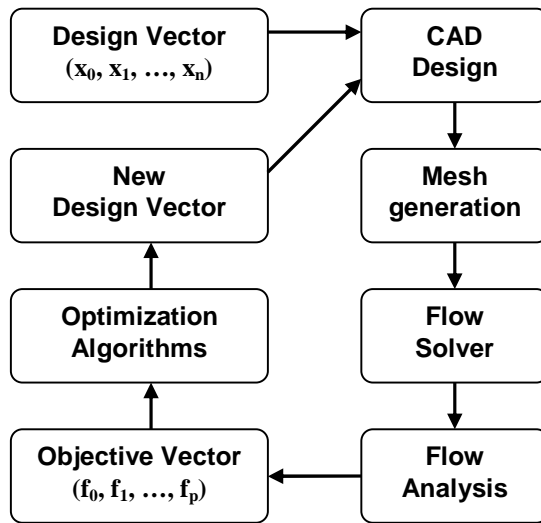


Figure 4: *ADONF*[®] flow process

C. Mesh influence on rig performance prediction

From the validation point of view, the main question about this optimization problem was to investigate the mesh influence on the predicted performances by RANS simulations. This question was important to be able to define the relevant mesh size and repartition over the calculation domain necessary to obtain accurate results for this kind of optimization problem. Relevant variables to predict the aerodynamic performances of a rig are the driving force F_r and the heeling moment M_c . Also, we have done a study of the output (F_r, M_c) obtained by RANS simulations as a function of the mesh refinement for a typical design of experiments (figure 5). The same set of 32 configurations representatives of all situations were computed by RANS simulations on three different meshes. The base mesh was composed of 31 000 grid points. The coarse mesh is approximately composed by cells four times larger than the base mesh and the fine mesh by cells four times smaller with approximately 120 000 grid points. As may be seen on the figure below, between the coarse and the base meshes differences are not negligible (around 10%) but they are considerably reduced between the base and the fine meshes (around 2%). This is true for all range of heeling moment and driving force. This illustrate that aerodynamic performances reasonably converge to an asymptotic value when the mesh is refined. It has been concluded that results obtained on the base mesh were sufficient for optimization purpose. We should have in mind that we just need to be able to rank configurations not to predict absolute values of driving force or heeling moment.

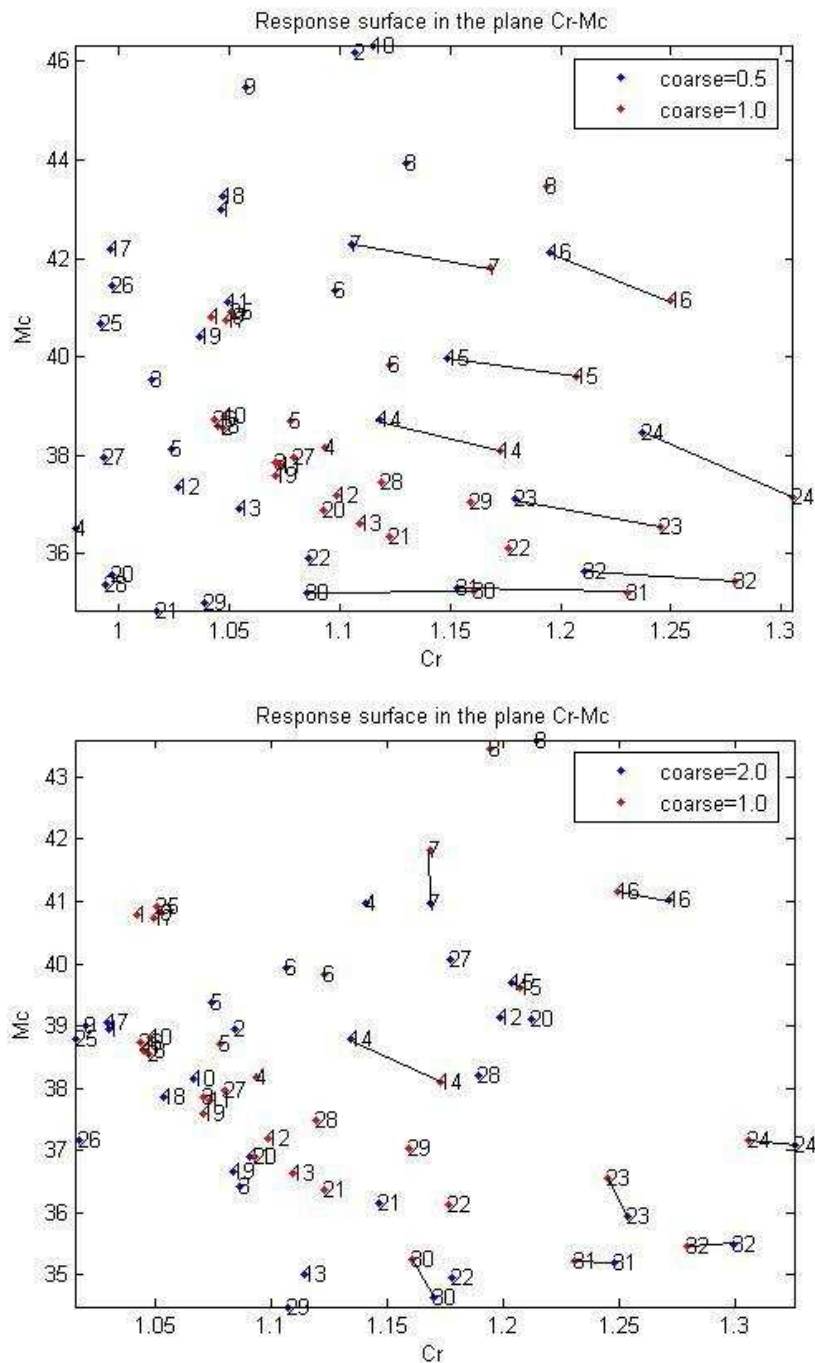


Figure 5: Mesh refinement influence on the response of the system in the objective plane (Cr, Mc) with the heeling moment versus the driving coefficient for a set of 32 typical three sails configurations. Red points are solutions obtained on the base mesh. Blue points are solutions obtained on the coarse mesh on first figure and on the fine mesh on second figure.

IV. Results and Discussions

A. Initial configuration

As a first step into the optimization process, we begin by defining the more realistic configuration of the Hydraplaneur rig at the chosen critical apparent wind angle $\beta = 75^\circ$. This is a three sails configuration with main design parameters given in the following table.

Table 3: three sails five-variable initial configuration

β	δ_{GV1}	δ_{GV2}	δ_{r2}	θ_1	θ_2	Fr	Mc
75	45	45	45	90	80	3.3	28

The flow field around this configuration is easily analyzed through visualizations from RANS/URANS simulations. On the following figures 6, where streamlines are visualized, we clearly see that for this critical apparent wind angle, the flow separate, on the suction side of the windward mainsail and leeward jib, on the pressure side of the leeward mainsail. This is due to the fact that the trim angle of sails is too small because of design limitations of the real yacht. These flow separations are leading-edge massive separations. The consequence of the separation on the pressure side of the leeward mainsail is a lower pressure on the pressure side of the leeward mainsail. The consequence of the windward mainsail separation is a lift and drag forces fluctuations on the rig. This force fluctuation may be analyzed by vortex shedding at the leading-edge of the windward mainsail, as is clearly observed on flowfield visualizations at different time in the period of the phenomenon not included in the paper. A careful observation of the pressure fields' shows that when the vortex shedding from the windward mainsail is convected toward the pressure side of the leeward mainsail it creates a low pressure region. This periodic low pressure region added to the already low pressure of the pressure side of the leeward mainsail may invert the pressure jump between both sides of the leeward mainsail. This phenomenon transposed to the real yacht may explain batten failure by a periodic excitation of the leeward mainsail with inversion of its cambered profile.

This analysis of a critical configuration through RANS/URANS simulations gives the motivation and the objective of the following optimization. The motivation will be to do not have batten failure on the real yacht. The objective will be to reattach the flow on the leeward mainsail and to attenuate the vortex shedding process on the windward mainsail which are both at the origin of the leeward sail periodic inversion of its cambered profile. If the previous analysis is good, it will be necessary and sufficient to attenuate the separation and the vortex intensity to do not have a pressure jump inversion on the leeward mainsail.

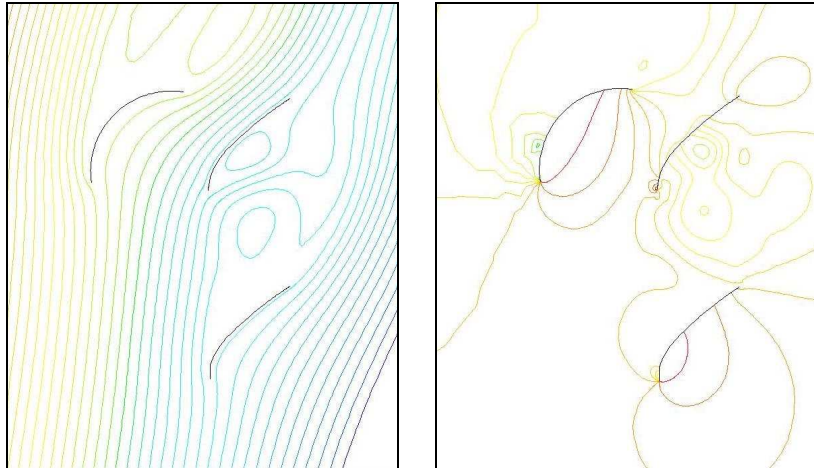


Figure 6: instantaneous streamlines and pressure field on the initial configuration

The analysis of this initial configuration suggests that a good mean to reduce flow separation and vortex shedding on the three sails configuration at this critical apparent wind angle should be to add a windward jib to

increase the flow deviation by the windward rig. In this four sails configuration, the added jib will play the role of a slat for the windward mainsail which is in a high angle of attack position in this configuration.

A four sail configuration has been design as a first trial to validate the idea of flow reattachment on the windward mainsail. We obtain a positive result as may be seen on the following figure 7. We see that separations on the suction side of the windward mainsail and on the pressure side of the leeward mainsail are largely limited by the added jib. The leading-edge vortex shedding on the windward mainsail has disappeared. On the next figure 8, which shows the lift history of both configurations, we see that mean lift has been increased and lift fluctuation has been largely reduced on the four sails configuration.

To conclude this part, we have found a plausible explanation to the instability problem of the Hydraplaneur in downwind conditions which mean batten failure on the real yacht. We have seen through a two-dimensional RANS analysis that it seems possible to increase further the critical apparent wind angle, and then the stability of the Hydraplaneur innovating rig, by adding a small windward jib which act as a slat of the windward mainsail. In the next section, we will investigate in more details the optimization of this unstable configuration of the Hydraplaneur. This will illustrate the potential of analysis, design and optimization of tools like *ADONF*[®] for any viscous flow situations with or without separated flow regions.

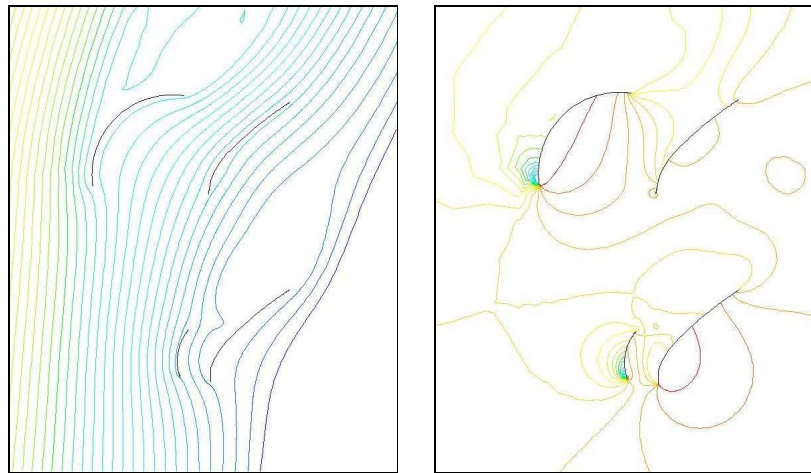


Figure 7: four sails configuration : (Left) instantaneous streamlines (right) instantaneous pressure field

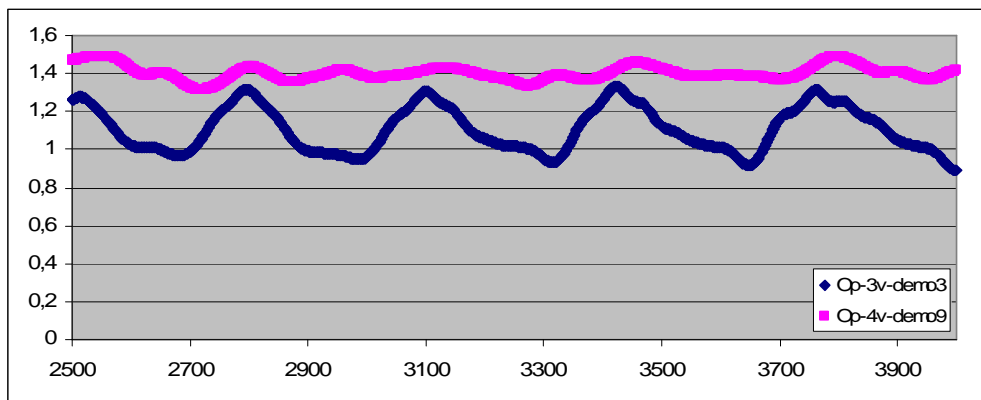


Figure 8: lift history on both configurations

B. Design of Experiments (DoE)

The first four sail design proposed in the previous section to resolve the identified stability problem was defined through a sailor and fluid researcher experience. In this section, to go further and try to investigate the power of Design of Experiments (¹⁸George E. P. Box, Norman R. Draper, ¹⁹Saporta G., Droesbeke J.-J., ²⁰Sado G. & M.C.), we will propose an optimization of the three and four sails configuration.

The two optimization problem considered are a five and a nine variables problems with one objective:

Three sails optimization problem: $Max(Fr(\delta_{GV1}, \delta_{GV2}, \delta_{f2}, \theta_1, \theta_2))$ with $\beta = 75^\circ$

Four sails optimization problem: $Max(Fr(\delta_{GV1}, \delta_{GV2}, \delta_{f2}, \theta_1, \theta_2, \delta_{f1}, c_{f1}, x_{f1}, y_{f1}))$ with $\beta = 75^\circ$

A constraint or second contradictory objective will be considered about the heeling moment Mc. In general, on sailing yacht, the heeling moment is bounded by the maximum righting moment which is a characteristic of a given yacht.

Two-level fractional factorial designs have been constructed to populate approximate response surfaces of a set of Hydraplaneur configurations around the initial design presented in the previous section. For the three sails configuration, we have done a first set of 17 RANS simulations completed by a second set of 27 RANS simulations resulting from the analysis of the first one. For the four sails configurations, a first set of 65 RANS simulations have been done. Main solutions found by these DoE that maximize the driving force Fr are detailed in the following tables 4, 5, 6.

Table 4: three sails five-variable DoE P13 optimal solutions

Run	δ_{GV1}	δ_{GV2}	δ_{f2}	θ_1	θ_2	Fr	Mc
1	50	50	50	95	95	3.87	25.9
2	50	40	50	95	75	3.98	27.1
4	50	40	50	75	95	3.81	26.4
12	40	40	50	95	95	3.83	28.4
16	40	40	50	75	75	3.85	29.4

Table 5: three sails five-variable DoE P23 optimal solutions

Run	δ_{GV1}	δ_{GV2}	δ_{f2}	θ_1	θ_2	Fr	Mc
4	47	45	52	90	90	4.18	28.0
6	52	45	52	90	80	4.21	26.3
7	47	40	52	90	80	4.24	27.9
12	52	40	52	80	80	4.17	26.5
23	50	42	55	85	85	4.36	26.6

Table 6: four sails nine-variable DoE P14 optimal solutions

Run	c_{f1}	δ_{GV1}	δ_{GV2}	δ_{f1}	δ_{f2}	θ_1	θ_2	x_{f1}	y_{f1}	Fr	Mc
5	4.0	50	40	80	50	95	75	-3.0	-6.6	5.78	31.6
17	4.0	50	50	80	50	95	95	-1.5	-4.6	5.08	28.2
34	4.0	40	40	80	50	95	95	-3.0	-6.6	6.13	35.8
40	4.0	40	50	80	50	75	75	-3.0	-6.6	5.84	34.4
47	2.0	50	50	80	50	95	75	-3.0	-4.6	5.11	30.3
53	4.0	50	50	80	50	75	95	-3.0	-6.6	5.88	31.3
54	4.0	50	40	80	40	75	75	-3.0	-6.6	4.95	34.6

An analysis of these solutions reveals that it seems highly favorable to increase trim angle of the windward mainsail and of the leeward jib.

The very best solutions obtained are presented in table 7. Analysis of the quadratic model has shown that the two mast angles (θ_1 , θ_2) have a small influence on the driving force and on the heeling moment compared to sheeting angles (δ_{GV1} , δ_{GV2} , δ_{r2}). The second DoE P23 defined after analysis of the results of the first DoE P13 propose a far better solution with run 23 of P23 which generate a 10% increase of the driving force for a small decrease of the heeling moment compared to run 2 of P13. This performance increase is obtained by increasing the leeward sheeting angle of the mainsail (+2°) and the jib (+5°). A detailed analysis of the flow solutions reveals that this driving force increase is the result of a smaller separation on the windward mainsail and on the leeward jib as may be seen on figure 9.

Table 7: Best solutions from all DoE

Run	δ_{GV1}	δ_{GV2}	δ_{r2}	θ_1	θ_2	Fr	Mc	Cl'
initial	45	45	45	90	80	3.3	28	0.20
P13 - 2	50	40	50	95	75	3.98	27.1	0.18
P23 - 23	50	42	55	85	85	4.36	26.6	0.18
P14 - 17	50	50	50	95	95	5.08	28.2	0.13

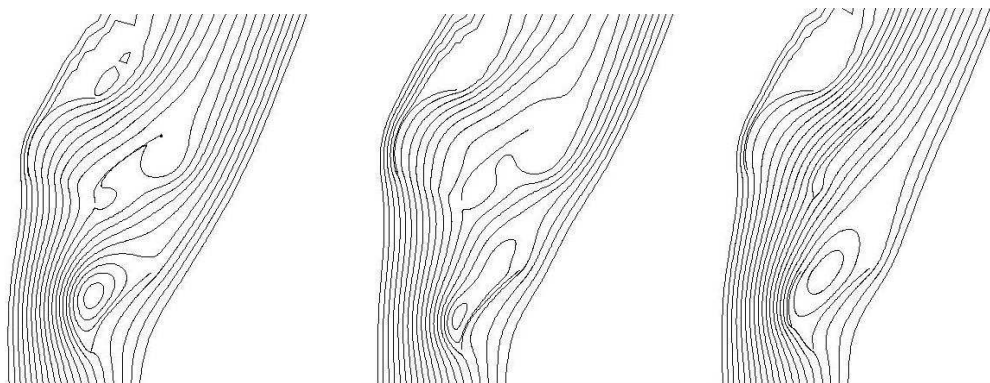


Figure 9: instantaneous flow streamlines (a) 3 sails run P1-2, (b) 3 sails run P2-23, (c) 4 sails run 17

Flow fields of these unstable configurations are highly complex with strong interaction between sails and massive flow separation in some configurations. These characteristics of the flow should imply a nonlinear behavior of the global rig. Also, it will be interesting to know if the global response surface of the problem which is in \mathbf{R}^5 for the three sails and \mathbf{R}^9 for the four sails configurations is composed by a unique optimum which may be found by a detailed optimization or if it is composed by multiple optimums with one global optimum. This is a common circumstance invoked to justify the usefulness of genetic algorithms for optimization problems but, as emphasized by ¹³Pulliam & al., it is not easy to found an aerodynamic problem with multiple optimums.

In the next section, we have tried to extract a sub-problem in \mathbf{R}^2 to be able to visualize the response surface.

C. Response surface of a sub-problem

A recurrent question about optimization problems is the choice of algorithms to find global optimum. Gradient methods are easy to program and fast enough to resolve but they have a drawback when the response surface of the optimization problem have multiple optimums. In this case, gradient methods only found the local optimum nearest to the initial design point. Based on this, many researchers explain that evolutionary algorithms like genetic methods are well adapted for problems with multiple optimums. These methods have also a drawback which is the large cpu time for real design problems.

The choice is easy when the response surface may be visualized but this is only possible for two variable response surfaces. This is highly restrictive. A related question rose from ¹³Pulliam (2003): Is it frequent in fluid dynamic design problems to have response surfaces with multiple optimums? It was not our objective to have an element of response to this general question when we have planned a detailed analysis of a subset of the design problem investigated in this paper. We have just decided to visualize the response surface of the three sails configuration of the Hydraplaneur with only two variables (sheeting angles of the two mainsails) to gain more insight in this problem. A set of 64 RANS simulations on this configuration has been done as illustrated in figure 10.

The response surface of the driving force as a function of the two mainsails sheeting angles is given in figure 11. This figure show that, in this particular fluid flow design problem, the response surface corresponding to the 2 selected variables has multiple optimums and a global one. This particular example found by hazard, shows the possible relevance of evolutionary algorithms for fluid design problems. If two variables problem have multiple optimums, it should be also the case for more complex design problems. An evolutionary algorithm has been used to found optimum design of the mainsail-jib problem in another paper (¹²Chapin).

Another interesting point about figure 11 is the fact that this approximate response surface for a subset of the initial design problem show that surrogate models of quadratic type may be insufficient to capture the complexity of this surface and then should not be sufficient to modelize real problems. This is an example of the general problem of the needed level of approximation to capture optimums through surrogate models.

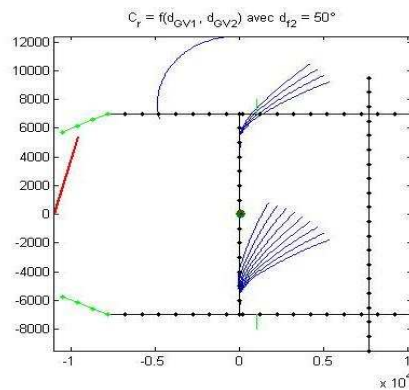


Figure 10: The three interacting lifting surfaces of the Hydraplaneur with the two mainsails sheeting angle varied to illustrate a sub-space of the DoE of the three sails five-variable problem.

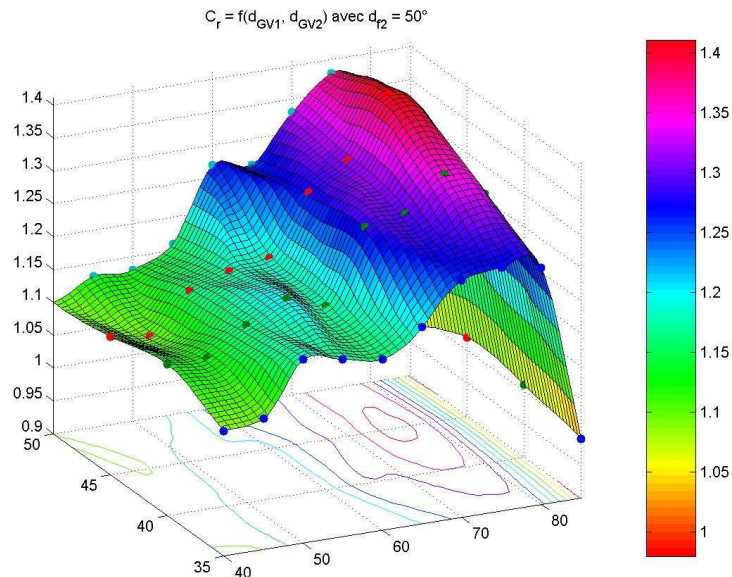


Figure 11: response surface example of a two-variable sub-problem for visual representation. Thrust coefficient versus sheeting angles of the two mainsails

D. Topological optimization results

When a trade-off is necessary between two contradictory objectives, it may be useful to Pareto frontiers in the objective space. Designs which are in the neighborhood of the Pareto frontiers are non-dominated designs. If we search for designs which maximize driving force and minimize the heeling moment, it is useful to plot all designs investigated in this (Fr, Mc) plane to evaluate best designs. This approach may be of particular interest to classify best designs obtained on the three sails configurations, and evaluate the potential gain of the topological optimization obtained by adding a windward jib to decrease the flow instability resulting from the high incidence angle of sails.

To have a global view on all the designs investigated, we have represented these designs in the objective space plane (Cr, Mc) with driving force versus heeling moment (figure 12). On this figure, we clearly see the Pareto frontier of each subset of the fractional factorial designs. A first Pareto frontier in blue is obtained with the first subset P13 with three sails. In the region of the complementary subset P23 always for three sails, we note a clear increase of the driving force for a given heeling moment in red. Next, the first subset of the four sails case P14 show an increase of the driving force for large heeling moment values but a decrease for lower ones. There is only a small heeling moment range [28-29] where four sails configurations may increase the driving force with a given heeling moment. This is partly the result of a total sail surface increase for the four sails configurations which results in a drift of the Pareto frontier toward higher heeling moment. A detailed analysis of the flow of four sails solutions shows that the windward jib, if well trimmed, may efficiently control the flow instability and results in a thrust increase. Also, it should be interesting to try to obtain an increase of the driving force with a constant sail surface and a smaller heeling moment for a four sail configuration. This may be done in the future.

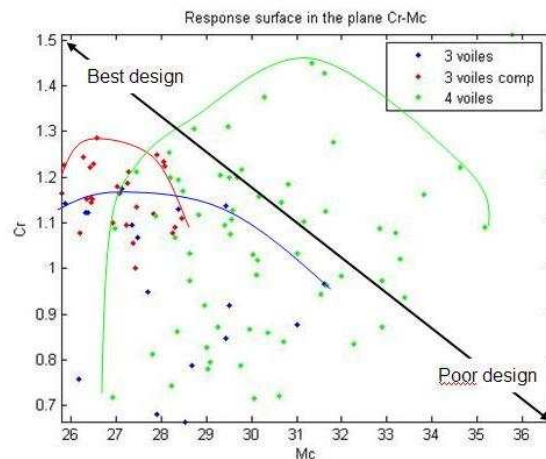


Figure 12: thrust coefficient versus heeling moment

E. Surrogate model of the three sails five variable case

As we have explained in a preceding section, quadratic surrogate models may be not sufficient to model the complex interaction of three or four sails in a wind. But in a well defined reduced area of the design space, surrogate models may be of interest to classify the relative importance of design variables for a given objective. Here, quadratic polynomials are used to model approximate response surfaces obtained through high-fidelity RANS simulations⁷ based on a two-level fractional factorial designs applied in a small area of the design space around one optimum found during DoE. In its general form, the quadratic polynomial model consists of $(n+1).(n+2)/2$ terms, i.e., 21 terms in the three sails five-variable configuration or 55 terms in the four sails nine-variables configuration as follow:

$$f(x) = \beta_0 + \sum_{i=1}^2 \beta_i x_i + \sum_{i=1}^2 \sum_{j \leq i}^2 \beta_{ij} x_i x_j + \sum_{i=1}^2 \beta_{ii} x_i^2 \quad (1)$$

Where β values are estimated by least squares methods. The surrogate model based on the second DoE for three sails based on 27 experiments is the following one for the driving force and the heeling moment:

$$F_r = 3.87 + 0.23 \delta_{f_2} + 0.018 \theta_1 - 0.026 \theta_2 + 0.024 \theta_1^2 + 0.017 \theta_2^2 \quad (2)$$

$$M_c = 26.88 - 0.61 \delta_{GV1} + 0.083 \delta_{GV2} - 0.28 \delta_{f_2} + 0.046 \theta_1 - 0.12 \theta_2 + 0.14 \delta_{f_2}^2 + 0.17 \theta_1^2 - 0.20 \delta_{GV1} \delta_{GV2} + 0.24 \delta_{GV2} \theta_2 \quad (3)$$

Order of magnitude and sign analysis of this surrogate model (equations 2 and 3) show that in the area of the design space considered here, the driving force is mainly a function of the trim angle of the leeward jib δ_{f_2} . The driving force is nearly independent to trim angles of both mainsails. The heeling moment is dependent to the trim angle of the windward mainsail, leeward jib, and of nonlinear terms. This kind of surrogate model around an optimum in downwind conditions may be useful for complex rigs trimming to help sailor to understand the complex flow which may take place in unstable situations with flow separation.

In the particular case shown here, we see on the surrogate model that if the sailor needs to reduce the heeling moment with urge he has to consider first the trim angle of the windward mainsail, then the trim angle of the leeward jib, etc... If the sailor just needs to increase the driving force, he just has to look for trimming the leeward jib.

V. Conclusion

In this paper, we have presented a flow optimization problem about interacting lifting surfaces typical to nautical and aeronautical aero-hydrodynamic platforms. We have resolved an optimization problem based on high fidelity RANS simulations, design of experiments and response surface technique. The optimization problem investigated was not only a parametric design problem but also a topological design problem with a change of the sail number in the optimization process. This topological optimization has been enabled by the newly developed simulation platform *ADONF*[®]. Results have shown the ability of these methods to find better designs in a reasonable time for small size problems (design space of dimension five to nine). They have also shown that evolutionary algorithms should be good candidates for fluid design problems because response surfaces with multiple optimums have been found on a subset of the design problem investigated. In the future, simulation capabilities will be extended to URANS for unsteady problems. From the optimization point of view, genetic algorithm like NSGA-2 and SPEA will be integrated into *ADONF*[®] to investigate multi-objective optimization in fluid mechanics.

References

¹A. J. Keane and P. B. Nair, "Computational Approaches for Aerospace Design: The Pursuit of Excellence", John-Wiley and Sons, ISBN 0-470-85540-1, 2005

²MARCHAJ, C. A., "Sailing Theory and Practice", McGraw-Hill, New York, 1962

3A. Gentry, The aerodynamic of sail interaction, Proceedings of the Third AIAA Symposium on the Aero/Hydraulics of Sailing, Redondo Beach, California, 1971

4A. Gentry, A Review of Modern Sail Theory, Proceedings of the Eleventh AIAA Symposium on the Aero/Hydraulics of Sailing, Seattle, Washington, 1981

⁵Milgram, J. H., "Sail force coefficients for systematic rig variations", Transactions of the Society of Naval Architects and Marine Engineers, 1971

⁶Korpus, R., "Performance Prediction without Empiricism: A RANS-Based VPP and Design Optimization Capability," Richard Korpus, 18th Chesapeake Sailing Yacht Symposium, Annapolis, MD, 2007

⁷Korpus, R., "Reynolds-Averaged Navier-Stokes in an Integrated Design Environment," Richard Korpus, Madrid Diseno de Yates, Madrid, 2004

⁸Chapin, V.G, "Twin rig of the Hydraplaneur", Contract report n°2002-2

⁹Chapin, V. G., Neyhousser, R., Jamme, S. Dulliand, G., Chassaing, P., "Sailing Yacht Rig Improvements through Viscous CFD", *17th Chesapeake Sailing Yacht Symposium*, Annapolis, Maryland, USA, March 2005

¹⁰Chapin, V. G., S. Jamme, P. Chassaing, "Viscous CFD as a relevant decision-making tool for mast-sail aerodynamics", *Marine Technology*, **42**(1), 1-10, 2005

¹¹Chapin V.G., Neyhousser R., Dulliand G., Chassaing P., "Analysis Design and Optimization of Navier-Stokes Flows around Interacting Sails", *Madrid Design Yacht Symposium*, Madrid, Espagne, 30-31 March 2006

¹²V.G. Chapin, R. Neyhousser, G. Dulliand, P. Chassaing, "Design Optimization of interacting sails", International Conference on Innovation in High Performance Sailing Yachts, RINA, Lorient, France, 29-30 May 2008

¹³Pulliam, T.H. Nemec, M. Holst, T. Zingg D.W., "Comparison of Evolutionary Methods for Multi-Objective Viscous Airfoil Optimizations, AIAA paper 2003-0298, Reno, USA, 6-10 January, 2003

¹⁴Queipo, N.V. & al., "Surrogate-based analysis and optimization", *Progress in Aerospace Sciences* 41 (2005) 1-28

¹⁵Mack, Y., Haftka, R.T., Segal, C., Queipo, N. and Shyy, W., "Computational Modeling and Sensitivity Evaluation of Liquid Rocket Injector Flow", AIAA-2007-5592, 43rd AIAA/ASME/SAE/ASEE Joint Propulsion Conference and Exhibit, Cincinnati, OH, July 8-11, 2007

¹⁶FLUENT 6.1 User's Manual, Fluent Inc 2003

¹⁷W. Song and A. J. Keane, "Surrogate-Based Aerodynamic Shape Optimization of a Civil Aircraft Engine Nacelle", *AIAA Journal* 45(10) pp. 2565-2574 ISSN 0001-1452, 2007

¹⁸George E. P. Box, Norman R. Draper, "Empirical Model-Building and Response Surfaces", Wiley Series in Probability and Statistics, 1987

¹⁹Saporta G., Droesbeke J.-J., "Plans d'expériences : Applications à l'entreprise", Editions Technip, 1997

²⁰Sado G. & M.C., "Les plans d'expériences", AFNOR, 2000